Density Functional Studies on Structure and Reactivity of Pd_n Clusters for n=1–13

Bulumoni Kalita and Ramesh Ch. Deka

Department of Chemical Sciences, Tezpur University, Tezpur 784028, Assam, INDIA

Abstract: Structure and relative stability of Pd_n clusters for n=1–13 in gas phase were investigated using density functional methods. The structures of Pd clusters were determined in terms of Pd-Pd bond length and the results are in very good agreement with experimental values. Stability of the clusters was determined from their relative energy values, binding energies and bond energies. We also calculated the reactivity of the Pd cluster using density functional based reactivity descriptor, Fukui function, which showed a decrease in reactivity with increasing cluster size.

1. Introduction

Metal clusters are nano dimensional materials which are an intermediate state of matter between molecular limit and bulk limit. Materials on nanoscale can suddenly show very different physical and chemical properties compared to what they show on macroscale. For example, opaque substances become transparent (copper) inert materials become catalysts (platinum) stable materials turn combustible (aluminium), solids become liquids at room temperature (gold), insulators become semiconductors (silicon) etc. This is due to the quantum size effects which describes the quantization of energy for the electrons in solids with great reductions in particle size. This effect does not come into play in going from macro dimensions while it becomes dominant in the nanometer size range. Other important aspects of the nanoclusters are high surface area to volume ratio and the dramatic change in their electronic structures. Both these effects lead to the greatly improved catalytic activity and aggressive chemical reactivity. Cluster properties are size dependent [2] and thus tunable. This brings the special interest in heterogeneous catalysis as well as for the synthesis of nano-structured materials.[1] Metals clusters have many potential applications in chemistry, physics and technology.

On the more applied side, Fe clusters promote the nitrogen plus hydrogen conversion into ammonia and platium clusters catalyze the process to the increase the octane grade of gasoline. Small clusters of Pt, Rh and Pd are used in automative exhaust systems to reduce toxic pollutants such as CO, NO, and hydrocarbons. Palladium, in particular, is a promising material as catalyst in various applications. For example, ultra-dispersed palladium clusters supported on alumina are found to be more active than Pd(111) single crystals in CO oxidation by oxygen.[3] In exhaust gas treatment, catalytic reduction of nitrogen monoxide with propane takes place on zeolite supported palladium clusters $[4,5\}^{i}$ and the extremely reactive NO is reduced by CO in presence of highly dispersed palladium clusters supported on γ-alumina [6] Moreover, ultra-dispersed supported palladium clusters of up to 2nm (150 atoms) in size act as highly active catalysts in hydrogenation processes [7], having much higher

selectivity in the conversion of triple to double bonds than that of bulk palladium.[8] It is important to determine the geometrical structure of transition metal clusters because it is a major factor in controlling their physical and chemical properties. This leads to an impressive effort towards a better understanding of the cluster properties such as geometry, bond strength and reactivity in several experimental and theoretical studies. Cluster properties such as ionization potential, electron affinity, reactivity[9-11] and magnetic behavior[12,13] are studied experimentally. Mass spectroscopy measurements observe the clusters of particular stability (magic numbers) [14] However, it is difficult to determine the geometrical structures of the clusters experimentally, especially in the gas phase. In this context theoretical calculations can complement experimental investigations in finding out the equilibrium geometry of the metallic clusters.

In the present work, most stable structures of Pd_n clusters for n=1–13 are investigated using density functional theory (DFT) with the aim of understanding the trends of characteristics (e.g., average bond length, binding energy per atom, reactivity etc.) with growing cluster size.

2. Computational Details

All the density functional calculations reported here were carried out using the DMol3 program [15,16] DMol3 is a widely used real-space first-principles cluster method, and has been successfully applied to many problems such as structural stability of molecular clusters, chemisorptions and surface reconstruction. It can perform accurate and efficient self-consistent calculation and structural optimization. The equilibrium structure can be obtained by relaxing atom until the energy gradients are deemed to be zero. DMol3 supports several exchange-correlation functionals. Among these, we have used the most popular nonlocal exchange-correlation functional, BLYP for the generalized gradient approximation (GGA). The exchange functional developed by Becke [17] is combined with the gradient corrected correlation functional by Lee, Yang and Parr [18] leading to the BLYP functional. In the local density approximation (LDA), the exchange-correlation energy of the uniform electron gas is obtained by adding the correlation functional developed by Vosko, Willk, and Nusair[19] in 1980 to the exchange functional, which is, apart from the perfactor, equal to the form found by Slater [20] in his approximation of Hartree-Fock exchange and was originally derived by Bloch and Dirac [21] in the late 1920s.

We have used the DNP basis set [22] in our calculations. DMol3 realizes the use of a double set of numerically tabulated basis functions. Generation of an entire second set of functions results in doubling the basis set size; this is referred to as a double-numerical (DN) set. Here the basis functions are represented numerically as values on atomic centered spherical polar mesh rather than as analytic functions (i.e., Gaussian orbitals), with cubic spline interpolations between mesh points. The angular portion of each function is the appropriate spherical harmonics Y_{lm} (Θ,Φ). The radial portion F(r) is obtained by numerically solving the atomic KS equations with the corresponding approximate exchange-correlation functional. The basis set can be significantly improved by adding higher angular momentum valence

polarization functions and also by core polarization functions. Additional basis functions, including polarization, are obtained by several procedures viz. DFT excited-state atom calculations, DFT atomic ion calculations or Hydrogenic orbitals. The occupied orbitals obtained from the neutral atom calculations comprise a minimal basis set for molecular systems. Greater variational flexibility beyond this minimal basis set is achieved by including orbitals from calculations for the atomic ions with a +2 charge, except for hydrogen where a nuclear charge of +1.3 is used. This basis functions provide a reasonable DN basis set. Adding a function on each atom with one angular momentum unit higher than that of its highest occupied orbital leads to a double numerical with polarization (DNP) basis set. The DNP basis is comparable to Gaussian 6-31G**basis set[23-25].

The stability of clusters is discussed in terms of the total interaction energy $V_{cluster}$, the binding energy E_b and the bond energy BE of the clusters defined as $V_{cluster} = (E_n - nE_1)$

$E_b = V_{cluster}/n$

$BE = V_{cluster}/m$

where n is the number of Pd atoms and m is the number of Pd-Pd bonds in the cluster, E_n is the energy of cluster Pd_n and E_1 refers to the atomic ground state (^1S).

3. Results and discussions

Full geometry optimizations have been carried out with DFT using relativistic LDA and GGA functionals for the lowest energy structures of Pd clusters, for $2 \leq N \leq 13$ [26-28]. The optimized geometries adopted by these Pd clusters are displayed in Figure 1. The symmetric point groups and the calculated average bond length of the clusters are given in Table 1.

Table 1. Calculated average bond lengths <d> (in Å) for various Pd clusters from relativistic LDA and GGA calculations and the corresponding point group symmetry.

		<d>/Å	
Cluster	PG	LDA	GGA
Pd_2	$D_{\infty h}$	2.445	2.596
Pd_3	D_{3h}	2.467	2.580
Pd_4	T_d	2.556	2.676
Pd_5	C_{4v}	2.562	2.683
Pd_6	O_h	2.599	2.697
Pd_7	D_{5h}	2.635	2.750
Pd_8	D_{2d}	2.610	2.736
Pd_9	C_{2v}	2.612	2.742
Pd_{10}	C_{3v}	2.623	2.749
Pd_{11}	C_{2v}	2.659	2.752
Pd_{12}	C_{5v}	2.670	2.770
Pd_{13}	I_h	2.659	2.751
bulk	—	—	2.750

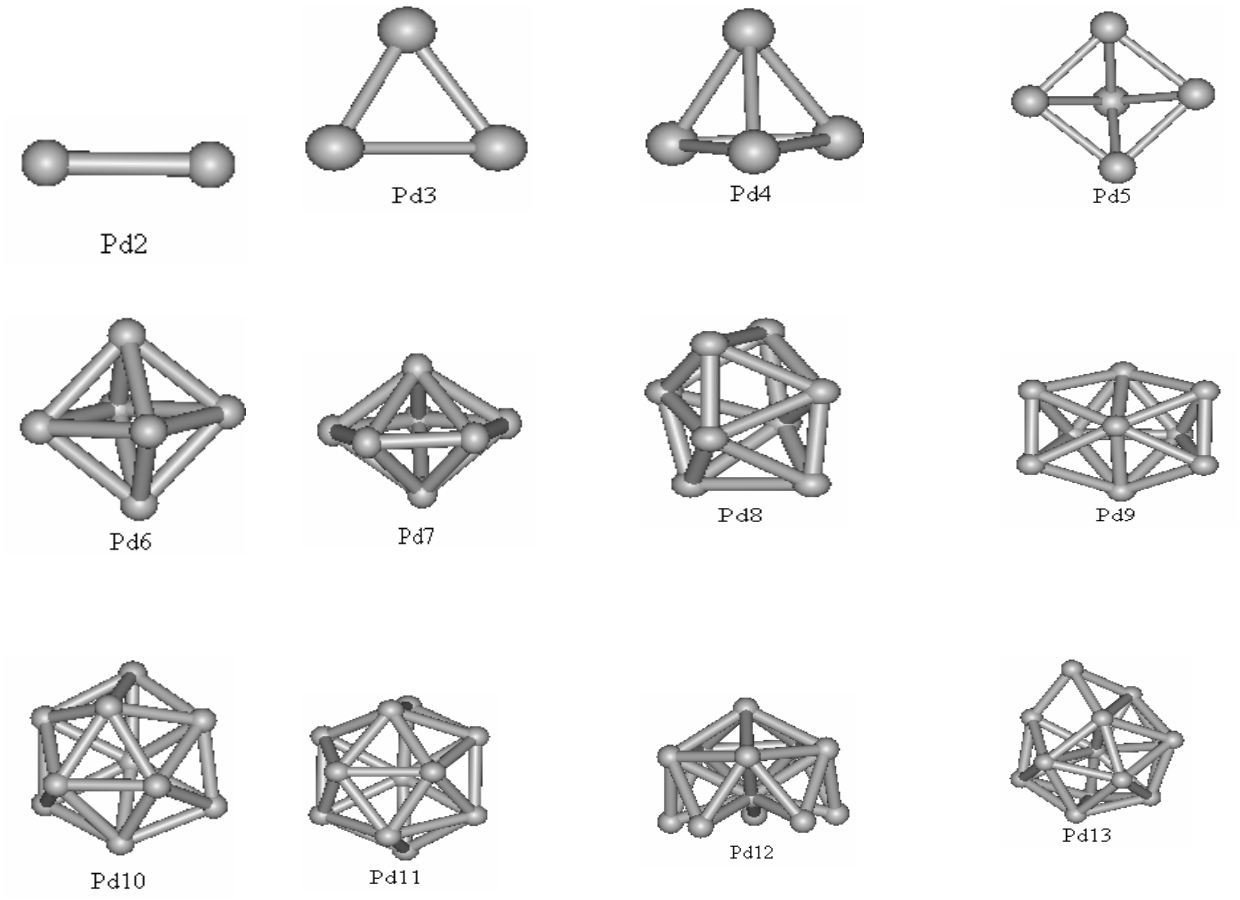

Figure 1. The geometries adopted by clusters Pdn, n=1-13, optimized by DFT using VWN and BLYP exchange-energy functionals.

The Pd_2 dimer is optimized with a symmetric point group of $D_{\infty h.}$ The Pd_3 trimer forms an equilateral triangle in D_{3h} symmetry. The optimization of Pd_4 gives a tetrahedron in T_d symmetry. Pd_5 is optimized with C_{4v} symmetry. The lowest energy structure of Pd_6 is an octahedron in O_h symmetry. The most stable isomer of Pd_7 shows a decahedral structure with D_{5h} symmetry. The lowest energy for Pd_8 is found in D_{2d} symmetry. The most stable structure of Pd_9 can be described as a decahedron or equivalently, as a portion of an icosahedron in C_{2v} symmetry. Decahedral pattern of Pd_{10} forms the most stable isomer with C_{3v} symmetry. The most stable structure of Pd_{11} is found for the structure in C_{2v} symmetry. An icosahedron with one vertex removed in C_{5v} symmetry gives the most stable structure of Pd_{12}. The icosahedron with I_h symmetry is most stable for Pd_{13} cluster.

In Figure 2. the average Pd-Pd bond length is plotted as a function of cluster size for the different exchange-correlation functionals. Each value corresponds to the statistical average of the different values of Pd-Pd bond

lengths calculated in different Pd_n, n=1-13 clusters for every value of n (the number of atoms in the cluster). The values of the bond lengths calculated with the LDA method are found to be almost similar with those of the SIESTA results of Rogan *et al [26]* **Error! Bookmark not defined.** For the dimmer, the bond length is found to be 2.45Å which is in good agreement with the accepted value of 2.48Å [19,30]. The bond length increases to a value of 2.66Å for the Pd_{13}. The results obtained from the LDA calculations are slightly shorter than those of Nava et al. and Kumar and Kawazoe[31]. The values for the bond lengths calculated with the GGA approach considerably overestimates the results of the LDA approach and also for the smaller sized clusters these values are found to be quite higher than those reported by Kumar and Kawazoe [30].. The average bond length results of both LDA and GGA method are almost similar with those of Krüger et al. [32] The bond distances found with the GGA functional are about 0.1- 0.15Å longer than those with the LDA, almost independent of the cluster size in agreement with the results of Krüger et al. [32] As an overall trend, the bond lengths increase with cluster size irrespective of the exchange-correlation energy functional used in the DFT calculation.

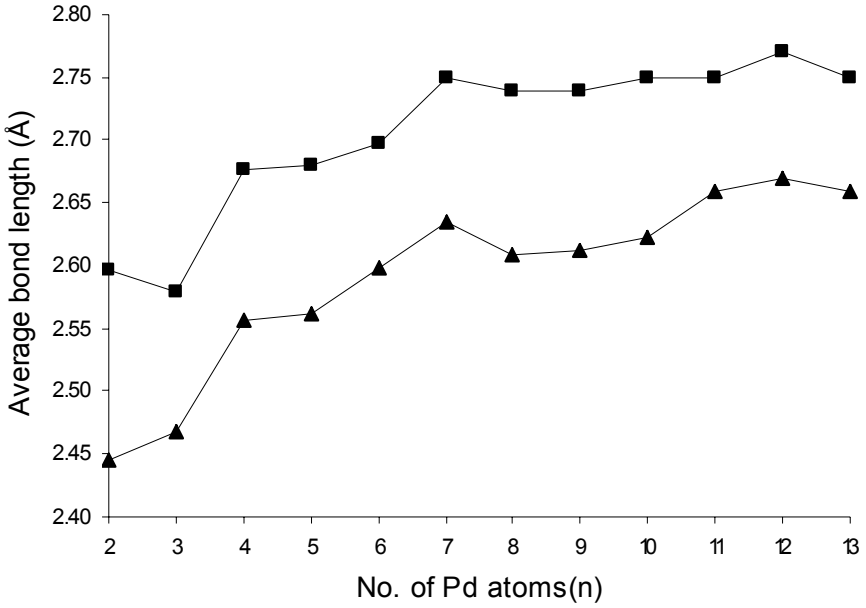

Fig. 2. Non-relativistic LDA (triangles) and GGA (squares) results of average bond lengths of clusters Pdn, n=1-13, as a function of the cluster size.

In Figure 3. we display the variation of the average bond lengths of the Pd_n, n=1-13 clusters with the average coordination number. The average coordination number is defined as sum of the coordination numbers of all n atoms of a cluster divided by n. The relation of bond length and average coordination number is found to be linear.

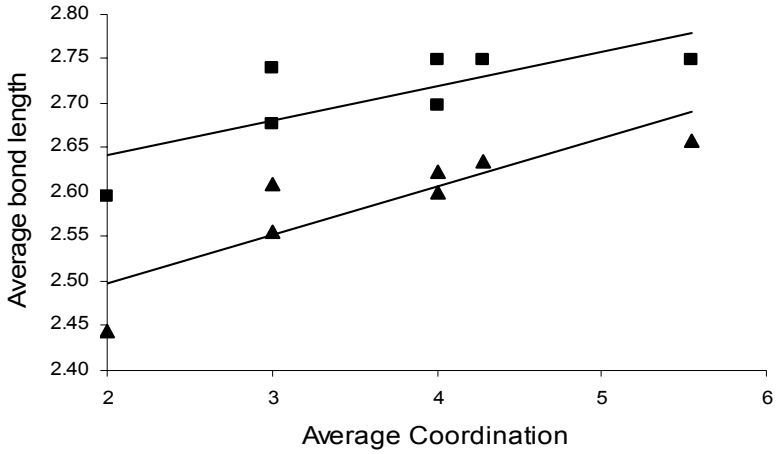

Figure 3. LDA(triangles) and GGA(squares) results for the average bond lengths as a function of average coordination.

The relative stability of the Pd clusters is investigated in terms of the evolution of the binding energy E_b. The total energy, the cluster energy, the binding energy and the bond energy of the clusters are given in the Table 2. The values of binding energy in both the LDA and GGA method increase with the cluster size. It shows that the stability of the clusters increases with the size of the clusters. The cluster energy and the binding energy values obtained with the GGA method agree well with the Voter & Chen [33] and Murell & Mottram[34]. These values are found to be little less than the results of [27,30] whereas the corresponding LDA results are quite higher. The binding energy for the Pd dimer, calculated with the GGA method is found to be 1.12 eV, which in close agreement with the trustworthy value (1.03 ± 0.16 eV)[35,36] The results show that even if the binding energies increase with increasing cluster size, the bond energies decrease with an exception for Pd_8 and Pd_{13}. This is in agreement with the statement of the bond energy conservation principle [37]. Our results for the binding energy as a function of cluster size are shown in Figure 4. From the graph it is seen that there is a dip in the vicinity of n=13, which corresponds to a region of enhanced stability (magic number).

We also calculated the first and second energy differences, $\Delta^{(1)}E$ and $\Delta^{(2)}E$ respectively defined as

$$\Delta^{(1)}E = E_b(n) - E_b(n-1)$$

$$\Delta^{(2)}E = E_b(n-1) - E_b(n+1).$$

The difference in E_b and $\Delta^{(1)}E$ gives the change in stability of the clusters from the bulk limit while a minimum of $\Delta^{(2)}E$ indicates an enhanced stability of a cluster relative to its heavier and lighter neighbors. Actually $\Delta^{(2)}E$ is a measure of stability of the clusters which is in general is correlated with experimental mass spectral intensities, rather than with the binding energy [30]. The second energy differences are plotted as a function of cluster size in Figure 5. Large negative minima of $\Delta^{(2)}E$ corresponds to the most stable Pd clusters. Both of the LDA and GGA values for $\Delta^{(2)}E$ are shown in Figure 5 identify Pd_4, Pd_6, Pd_8 and Pd_{10} as the most stable structures.

Table. 2. The total energy, the cluster energy, the binding energy and the bond energy of various clusters Pd_n, n=1-13 using exchange-energy functionals VWN (LDA) and BLYP (GGA).

Cluster	Total energy (eV)		Cluster energy (eV)		Binding energy (eV/atom)		Bond energy (kcal/mol)	
	LDA	GGA	LDA	GGA	LDA	GGA	LDA	GGA
Pd	-139126.44	-139266.85	—	—	—	—	—	—
Pd_2	-278254.62	-278534.81	-1.74	-1.12	-0.87	-0.56	-40.08	-25.88
Pd_3	-417384.43	-417803.89	-5.1	-3.36	-1.7	-1.12	-39.18	-25.82
Pd_4	-556514.38	-557073.07	-8.61	-5.69	-2.15	-1.42	-33.1	-21.85
Pd_5	-695643.69	-696341.7	-11.47	-7.47	-2.29	-1.49	-33.07	-21.55
Pd_6	-834773.75	-835610.27	-15.09	-9.2	-2.51	-1.53	-29	-18.57
Pd_7	-973903.13	-974879.29	-18.03	-11.38	-2.58	-1.63	-25.99	-16.4
Pd_8	-1113033.06	-1114148.26	-21.51	-13.5	-2.69	-1.69	-27.56	-17.3
Pd_9	-1252162.94	-1253417.18	-24.95	-15.58	-2.77	-1.73	-25.02	-15.62
Pd_{10}	-1391292.96	-1392686.15	-28.53	-17.7	-2.85	-1.77	-24.37	-15.12
Pd_{11}	-1530422.88	-1531955.09	-32	-19.8	-2.91	-1.8	-23.81	-14.73
Pd_{12}	-1669552.98	-1671224.07	-35.66	-21.92	-2.97	-1.83	-22.85	-14.04
Pd_{13}	-1808683.06	-1810493.24	-39.3	-24.25	-3.02	-1.87	-23.85	-14.72
bulk	—	—	—	—	—	—	—	-15.00

We used the density functional based reactivity descriptors to investigate the reactivity of the Pd clusters. The reactivity of the clusters are defined in terms of the Fukui functions, f^+ which are evaluated using Hirshfeld population analysis (HPA) and Mulliken population analysis (MPA) schemes. The average of Fukui functions are shown in Table 3. The values of the average Fukui functions, f^+ calculated with the LDA and GGA methods are found to be same.

Figure 6 displays the variation of the reactivities with the number of atoms in the Pd clusters. It is observed that the reactivity decreases as the number of atoms increases in the cluster. This decrement in reactivity in Pd_n is fast for n=1 to 6 while it is slow from n=7 to 11 and ultimately it becomes constant for n=12 and 13.

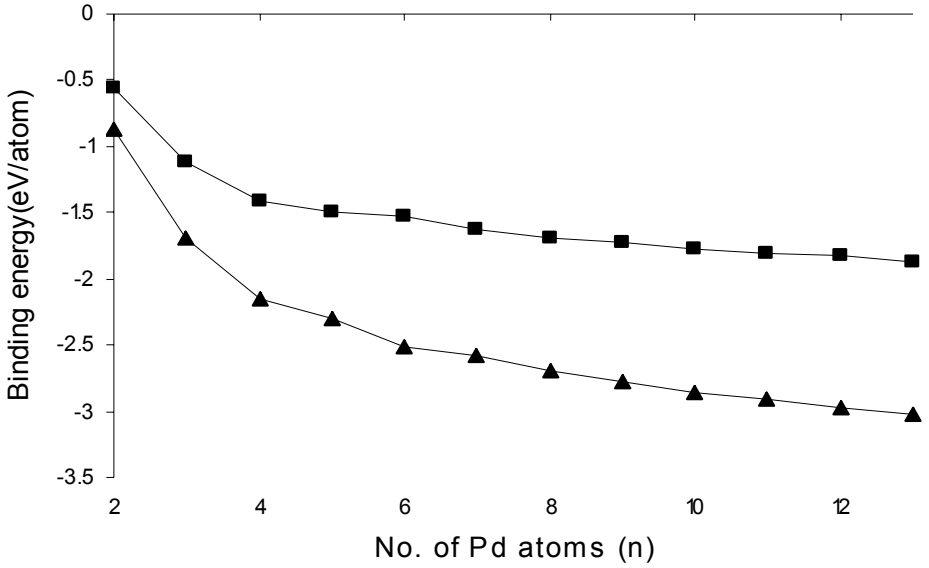

Figure 4. Energy per atom, as a function of cluster size. The triangles and the squares correspond to the LDA and the GGA results respectively.

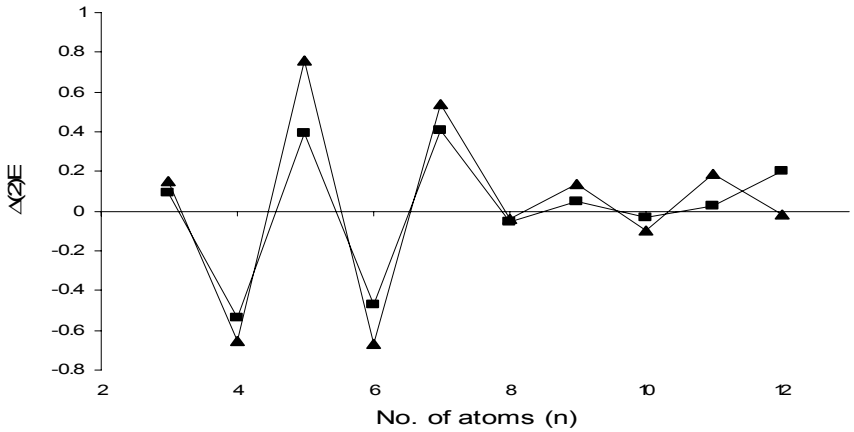

Figure 5. LDA(triangles) and GGA(squares) results of second energy difference

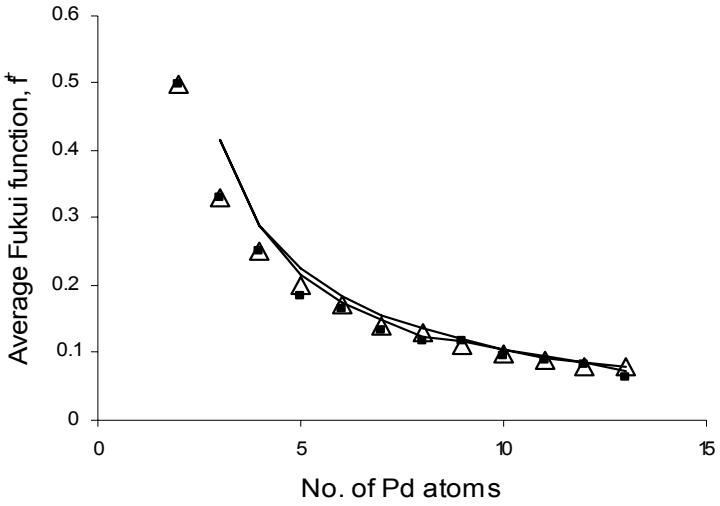

Figure 6. Variation of average Fukui functions f^+ obtained from LDA (triangles) and GGA (squares) with cluster size.

Table 3. Average Fukui functions (f+) of Pd_n, n=1-13, clusters using LDA and GGA methods.

Cluster	Average Fukui function (f^+)	
	LDA	GGA
Pd	1	1
Pd_2	0.5	0.5
Pd_3	0.33	0.33
Pd_4	0.25	0.25
Pd_5	0.2	0.2
Pd_6	0.17	0.17
Pd_7	0.14	0.14
Pd_8	0.13	0.13
Pd_9	0.11	0.11
Pd_{10}	0.1	0.1
Pd_{11}	0.09	0.09
Pd_{12} & Pd_{13}	0.08	0.08

4. Conclusion

With the help of density functional theoey we have calculated the Pd-Pd bond lengths of palladium nanoparticles of upto 13 atoms. The results show a clear contraction of the average bond lengths with decreasing cluster size irrespective of the functionals used for calculation. This is in very good agreement with the previous theoretical and experimental studies. It is also seen from the results that the bond distances obtained from LDA calculations are more accurate than those from GGA calculations. The stability of the clusters is measured in terms of cluster energy, binding energy and bond energy. Both GGA and LDA calculation showed that the binding energies increase whereas the bond energies decrease with the cluster size. It is observed that GGA calculation is more reliable than that of LDA for the study of stability of clusters. Also from the second energy differences we have found Pd_4, Pd_6, Pd_8 and Pd_{10} as the most stable clusters. The reactivity of the clusters are studied with the help of average Fukui functions f^+, which is found to decrease with increasing cluster size.

Acknowledgement

The authors thank the Council for Scientific and Industrial Research, New Delhi for financial support.

Referecnes:

1. L. J. Jongh, Physics and Chemistry of Metal Cluster Compounds, Kluwar Academic Publishers, Dordrecht. 1994.
2. N. Rösch and G. Pacchioni, in Clusters and Colloids—From Theory to Aoolications, edited by G. Schmid (chemie, Weinheim, 1994), p. 5.
3. I. Stara, V. Nehasil, V. Matolin, *Surf. Sci.*173, 331 (**1995**).
4. S. Tanabe, H. Matsumoto, *J. Mater. Sci. Lett*. 13, 1540 (**1994**).
5. H. Matsumoto, S. Tanabe, J. Phys. Chem. 99, 6951 (**1995**).
6. M. Valden, J. Aaltonen, E. Kuusisto, M. Pessa, C. J. Barnes, *Surf. Sci*. 193, 307 (**1994**).
7. M. Che, C. O. Bennett, *Adv. Catal*. 36, 55 (**1989**).
8. G. D. Zakumbaeve, N. F. Toktobaeva, A. G. Kubasheva, I. G. Efremenko, Neftechimija, 3 (**1994**)
9. Ervin, K. M.; Ho, J.; Lineberger, W. C. *J. Chem. Phys.* 89, 4514 (**1988**).
10. Fayet, P.; Kaldor, A.; Cox, D. M., *J. Chem. Phys.* 92, 254 (**1990**).
11. Ren, X.; Hintz, P. A.; Ervin, K. M. *J. Chem. Phys.* 99, 3575 (**1993**).
12. Pacchioni, G.; Bagus, P. S.; Parmigiani, F. Cluster Models for Surface and Bulk Phenomena, NATO ASI series B, Physics; Plenum: NewYork, 1992; Vol. 283. p 67
13. Douglass, D. C.; Bucher, J. P.; Bloomfield, L. A. *Phys. ReV. B* 45, 6341 (**1992**).
14. Koutecky, J.; Fantucci, P. *Chem. Rev.* 86, 539 (**1986**).
15. B. Delley, *J. Chem. Phys.* 113, 7756 (**2000**).
16. B. Delley, *J. Chem. Phys.* 92, 508 (**1990**).
17. A. D. Becke, *Phys. Rev. A* 38, 3098 (**1988**).
18. C. Lee, W. Wang and R. G. Parr, *Phys. Rev.* 37, 785 (**1988**).
19. S. H. Vosko, L. Willk, and M. Nusair, *Can. J. Phys.* 58, 1200 (**1980**).
20. J. C. Slater, *Phys. Rev.* 81, 385 (**1951**).
21. P. A. M. Dirac, *Proc. Cambridge Phil. Soc.* 26, 376 (**1930**).
22. B. Delley, *J. Chem. Phys*., 92, 508 (**1990**).
23. C. W. Bock, M. Trachtman, *J. Phys.*

Chem. 98, 95 (**1994**).
24. M. S. Gordon, *Chem. Phys. Lett.* 76, 163 (**1980**).
25. W. J. Hehre, R. Ditchfield, J. A. Pople, *J. Chem. Phys.* 56, 2257 (**1972**).
26. José Rogan, Griselda García, Juan Alejandro Valdivia, W. Orellana, A.H. Romero, Ricardo Ramírez and Miguel Kiwi, *Phys. Rev. B* 72, 115421 (**2005**).
27. Wenqin Zhang, Qingfeng Ge and Lichang Wang, *J.Chem. Phys.* 118, 5793 (**2003**).
28. Paola Nava, Marek Sierka and Reinhart Ahlrichs, *Phys. Chem. Chem. Phys*. 5, 3372 (**2003**).
29. J. Ho, K. M. Ervin, M.L. Polak, M.K. Gilles and W.C. Lineberger, *J. Chem. Phys.* 95, 4845 (**1991**).
30. J. R. Lombardi and B. Davis, *Chem. Rev. (Washington, D.C.)* 102, 2431 (**2002**).
31. Vijay Kumar and Yoshiyuki Kawazoe, *Phys. Rev. B* 66, 144413 (**2002**).
32. Sven Krüger, Stefan Vent, Folke Nörtemann, Markus Staufer and Notker Rösch, J. Chem. Phys. 115, 2082 (**2001**).
33. A.F. Voter and S.Chen , in Characterization of Defects in Materials, edited by R. W. Siegel, J. R. Weertman, and R. Sinclair, MRS Symposia Prooceedings No. 82 (Materials Research Sociery, Pittsburgh, 1987), p. 175.
34. J. N. Murrell and R.E. Mottram, Mol. Phys. 69, 571 (**1990**).
35. I. Shim and K. A. Gingerich, J. Chem. Phys. 80,5107 (**1984**).
36. M. D. Morse, Chem Rev. 86, 1049 (**1986**).
37. Gabriele Valerio and Herve Toulhoat, J. Phys. Chem. 100, 10827 (**1996**).